Green Chemistry

Controlled assembly of secondary keratin structures for continuous and scalable production of tough fibers from chicken feathers

Journal:	*Green Chemistry*
Manuscript ID	GC-ART-11-2019-003896.R2
Article Type:	Paper
Date Submitted by the Author:	27-Jan-2020
Complete List of Authors:	Mu, Bingnan; University of Nebraska-Lincoln, Textiles Hassan, Faqrul ; University of Nebraska-Lincoln, Textiles Yang, Yiqi; University of Nebraska-Lincoln, Biological Systems Engineering

Controlled assembly of secondary keratin structures for continuous and scalable production of tough fibers from chicken feathers

Bingnan Mu[a], Faqrul Hassan[a] and Yiqi Yang[a,b,c,*]

[a] Department of Textiles, Merchandising and Fashion Design, 234, HECO Building, University of Nebraska-Lincoln, Lincoln, NE 68583-0802, United States

[b] Department of Biological Systems Engineering, 234, HECO Building, University of Nebraska-Lincoln, Lincoln, NE 68583-0802, United States

[c] Nebraska Center for Materials and Nanoscience, 234, HECO Building, University of Nebraska-Lincoln, Lincoln, NE 68583-0802, United States

* Corresponding Author. Tel: +001 402 472 5197; Fax: +001 402 472 0640; E-mail: Yiqi Yang <yyang2@unl.edu>;

Abstract

Tough keratin fibers from chicken feathers have been produced continuously via controlled assembly of secondary protein structures. Though research for utilization of keratinous wastes began decades ago, very few regenerated products with high quality were developed due to damages to the primary structures during extraction and poor recovery of the secondary structures in the regenerated materials. Fibers have the highest quality requirements among the regenerated keratin products, including high toughness and resistance to repeated launderings, and high toughness. Our group developed regenerated keratin fibers on lab-scale previously. However, the regenerated keratin had poor spinnability with low recovery of secondary protein structures. As a result, keratin fibers could not be produced continuously and their properties especially the wet strength were not acceptable. In this paper, high drawing ratios of keratin fibers on a continuous line have been achieved via stepwise oxidation and drawing technology. This technology resulted in controlled assembly of disulfide crosslinkages, optimum recovery of the secondary structures, satisfactory mechanical properties and scalable production of keratin fibers. Furthermore, the use of inexpensive chemicals makes continuous keratin fiber production developed in this work affordable for scale-up. The technology developed for continuous production of tough keratin fibers has a high potential for the development of high quality regenerated products from other cysteine-containing protein materials.

Keywords: Keratin fibers; Continuous production; Secondary structures; Disulfide bonds assembly

Introduction

Research on the preparation of high-end materials through green synthesis technology has received much attention in recent years [1-3]. Meantime, there is a trend for utilizations of natural polymers and fibers for green processing[4] because such utilizations not only reduce environmental pollution, but also introduce some unique properties to final products such as low density, moisturizing and biocompatibility[5, 6]. Natural fibers' implementations in various areas of materials science and technology are becoming even broader. Recent examples include production of nonwoven membrane from bamboo fibers[7], regenerated fibers produced from whole biomass[8] and fully recycling and utilization of waste cotton[9]. Utilizations of wastes to decrease the pollutions and increase sustainability are also crucial [6, 10]. In terms of textile fibers, more than 80 million tons of synthetic fibers are produced every year globally [11]. Almost all synthetic fibers are petroleum-based and hardly degradable in the environment [12]. Therefore, it is urgent to find sustainable, environmentally responsible and affordable alternatives to replace petroleum-based fibers [13, 14].

Keratinous wastes, especially poultry feathers, are abundant, safe, cost-effective and readily available materials for fiber production [15]. Among all poultries, chicken consumption is the largest worldwide [16]. With an annual chicken consumption of about 65 million tons and a subsequent generation of 5 million tons waste chicken feathers worldwide annually [17], the potential production of protein fibers from chicken feathers is already 2.5 times higher than the current output of both wool and silk. Chicken feathers contain keratin content as high as 90-92% [18]. Having linear polymeric backbones and an average molecular weight higher than 10 kDa [19], feather keratin meets requirements of molecular structures for fiber spinning. With around 7% cysteine served as crosslinking sites, feather keratin is expected to possess good tensile

properties and aqueous stabilities [20]. Regenerated fibers from feather keratin are likely to have smooth touch, moisture transmission and thermal insulation because of similar chemical structures to those of wool and silk [14].

Unsuccessful continuous fiber production results from the difficulty in keratin extraction from feathers, incomplete re-dissolution of keratin, limited alignment of molecular chains of protein and inefficient recovery of disulfide crosslinkages. For a long period of time, strong alkali solutions were used to dissolve and extract keratin [21]. However, high pH not only hydrolyzed protein backbones but also reduced amounts of sulfhydryl groups of keratin [22, 23]. As a result, it was impossible to produce high-quality fibers. Since ionic liquids have been used to extract keratin from wastes [24, 25], such liquids were used to dissolve keratin for spinning. However, the properties of obtained fibers were not satisfactory [26] because keratin cannot fully dissolve in ionic liquids. While ionic liquids could break ionic interactions and hydrogen bonds, they are not able to interrupt disulfide bonds and hydrophobic interactions among keratin molecules. Our research group developed the non-destructive extraction system and first regenerated keratin fibers from chicken feathers on a lab-scale [27]. However, such fiber spinnings lacked essential techniques to efficiently recover the disulfide bonds and secondary structures. As a result, the spinnability of keratin fibers was not good. As a result, linearity of the regenerated fiber was poor, distance between keratin chains was long and chance for formation of intermolecular disulfide crosslinkgaes was low. Resultant fibers had a large diameter, low strength, and poor flexibility. The tenacity of the regenerated fiber was only 50% of the original chicken feathers and strain was only 4%. In addition, the regenerated keratin fiber did not inherit good wet properties from chicken feathers. Although the research regarding the fiber production from keratinous waste began in the 1940s [28], there were hardly any efficacious methods developed to

continuously produce regenerated pure keratin fibers with high quality. The minimal requirement for fibers is to have stress and strain higher than 100 Mpa and 10%, respectively. To achieve above requirement, most research focused on either post crosslinking or addition of tough polymers such as PVA and cellulose into keratin fibers [26, 29-32].

This work focuses on the ready for scale-up production of quality keratin fibers on a continuous line. Specifically, we fine control the cleavages and assembly of disulfide linkages in keratin fibers during the continuous spinning for high recovery of protein secondary structures. To fine control the restorations of disulfide bonds, stepwise oxidation and drawing process have been designed on a continuous line. The detailed objectives are to establish disulfide crosslinkages, optimize the stretch and alignment of keratin molecules, and to improve the spinnability and properties of fibers. Finally, the keratin fibers from continuous production are comparable to feathers in mechanical properties and wet properties.

Experimental

Materials

Feather fiber corporation, Nixa, CO provided us chicken feather barbs with keratin content around 92%. Sodium periodate, urea and sodium carbonate were from Alfa Aesar (Haverhill, MA) with purities of 98%. Sodium dodecyl sulfate (SDS) with purity of 95%, cysteine with purity of 99.7%, mercaptoethnaol with purity of 99%, sodium hydroxide with purity of 98% and sodium bicarbonate with purity of 99.7% were purchased from VWR International (Radnor, PA). Hydrochloric acid was purchased from Macron Fine Chemicals (Radnor, PA) with purity of 36-38%. Sodium acetate with purity of 98% and acetate acid with ACS GR were purchased from EMD Millipore (Darmstadt, Germany). Zinc sulfate with purity of 99% was purchased from

Spectrum Chemical (New Brunswick, NJ). Phenylisothiocyanate and sodium sulfate with purity of 99% was purchased from TCI (Boston, MA). Acetonitrile was purchased from JT Baker (Radnor, PA) with putiry of 99.9%. Chemical reagents used in SDS-PAGE analysis, including LDS sample buffer (4×), Nupage 20× MES running buffer and NuPAGE 4–12% Bis-Tris gel, were purchased from Invitrogen, Inc (Grand Island, NY). Chemicals selected for continuous spinning were from perspectives of safety, non-toxicity, and degradability. For instance, SDS, used for keratin extraction and spinning dope preparation, has acceptable biodegradability [33]. However, the toxicity is still a concern for some chemicals used in this work. Nontoxic, degradable alternatives still need to be found for replacing current chemicals.

Keratin extraction from chicken feathers

The extraction of keratin from chicken feathers was conducted using an aqueous solution containing different amounts of urea and SDS. To determine the optimal recipe, viscosity of supernatant of extraction and keratin yield was measured. Detailed results are in Table S1. Finally, 2 M urea and 10% SDS based on the weight of feathers were chosen. 10% of cysteine was used to fully cleave the disulfide bonds in feathers for optimal keratin dissolution. Cysteine was used to extract keratin from chicken feathers because cysteine is a green reducing agent. According to the previous work, the pH of extraction solution was adjusted to 10.5 using 15 wt% NaOH solution [27]. The extraction was held for 12 hours at 70 ^{o}C. After the extraction, the dispersion was centrifuged at 9800 rcf for 20 min to obtain the supernatant which was further adjusted to the isoelectric point using hydrochloric acid accompanied by sodium sulfate to precipitate keratin. The precipitated keratin was further washed to remove impurities before vacuumed dried.

Preparation of keratin spinning dope

Spinning dope for continuous pilot-scale spinning was prepared by dissolving 27% of extracted keratin and 10% of SDS based on the weight of keratin in 0.2 M carbonate-bicarbonate buffer at pH of 8. To fully dissolve keratin and obtain the optimal molecular entanglement in solution, different amounts of reducing agents, mercaptoethanol, were added for controlled cleavage of disulfide bonds in keratin. Mercaptoethanol was used because further addition of cysteine to spinning dopes formed submicron cystine particles[34]. Such particles would deteriorate the properties of micron-level keratin fibers. Furthermore, cystine particles in keratin fibers could interfere with the quantification of disulfide linkages in keratin since such linkages were in the form of cystine.

Continuous wet spinning of keratin fibers using stepwise oxidation and drawing

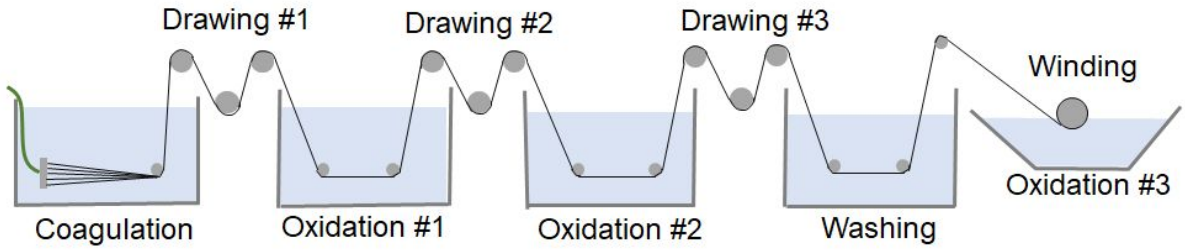

Figure 1. Diagram of wet spinning line on a pilot-scale employed with stepwise oxidation and drawing

Stepwise oxidation and drawing were applied to continuous wet spinning lines (ALEX JAMES AND ASSOC, US) for controlled assembly of disulfide bonds in keratin fibers. Stepwise oxidation and drawing can help improve the spinnability, alignment of keratin molecules, degrees of crosslinkages and ultimately fiber properties. Detailed design is demonstrated in Figure 1. Prepared keratin spinning dope was centrifuged before installed onto the spinning line. Keratin solution was extruded via a spinneret with multiple 50 μm-diameter holes to the

coagulation bath containing 15 wt% sodium sulfate, 5 wt% zinc sulfate and acetate buffer with pH 2. For each time, around 8,000 meters of fibers were spun using the same coagulation bath. The liquor ratio of coagulation bath to fibers each time was around 2,500:1. After each spinning, we added several drops of hydrochloric acid to adjust pH of coagulation bath back to 2 before the next spinning. At least for 9 times of fiber spinnings using the same coagulation bath, there were no significant differences in fibers' properties. Fibers from the coagulation bath were drawn for the first time before entering the first oxidation bath. The oxidation bath contained 4 g L^{-1} sodium periodate as the oxidation agents and acetate buffer with pH of 2. Oxidation temperature was 35℃ to ensure the fast disulfide bond assembly and fine fiber stretchability. Fibers then went through multiple drawings and oxidations before going to the washing bath. Multiple oxidation and drawing can help the establishment of disulfide bonds and ordered structures in keratin fibers. Due to the length limitation of current spinning line, two cycles of oxidation and drawing were conducted in our work. An increase in oxidation and drawing cycles could further improve fiber properties. The washing bath contained surfactants with concentrations from 1 g L^{-1} and acetate buffer with pH of 4. The temperature was 40 ^{o}C to ensure high washing efficiency. Reaching the final winding roller, the fibers went through the oxidation bath once again for the immobilization of ordered molecular structures in keratin fibers. The final speed of fiber collecting was 15 meters min^{-1}. The dry fibers obtained were dried in an oven at 85 °C for 1 h and later annealed at 125 °C for about 1 h. Annealing was done to improve the mechanical properties of the fibers.

Characterizations

Rheological properties of spinning dope

Shear stress (τ, Pa) of keratin spinning dopes with various concentrations of reducing agents was measured using a rotational rheometer, R/S plus (Brookfield, U.S.A.) for determination of consistency coefficient (K, Pa•s^n) and flow behavior index (n) based on equation 1. K is directly proportional to polymer viscosity in solution and n indicates the degree of molecular entanglement in solution. The smaller the value of n, the better the molecular entanglement. To precisely measure the rheological properties, 18 wt% of keratin solution was used.

$$\tau = K\dot{\gamma}^n \qquad \text{Equation 1}$$

where $\dot{\gamma}$ is the shear rate (s^{-1}) measured in the range of 0-1000 s^{-1}.

Molecular weight of keratin backbones

About 2 mg of feather and keratin fiber was dissolved in 100 μL of NuPAGE LDS sample buffer (4 ×) with excess mercaptoethanol, heated at 70 °C for 5 h. The solution was centrifuged prior to loading. Each sample of 10 μL was loaded into an individual slot of the gel. A molecular marker from Spectra Multicolor Low Range Protein Ladder was used. The molecular weights of the protein standard mixture ranged from 4.6 to 42 kDa.

Morphologies of fibers

The morphologies of keratin fibers were characterized using a Field-Emission Scanning Electron Microscope (Hitachi S4700 Field-Emission SEM).

Mechanical properties

Keratin fibers were conditioned at 21 °C and 65% relative humidity for 24 h prior to tests. Tensile properties of keratin fibers were obtained according to ASTM standard D-3822 using an Instron tensile testing machine (Norwood, MA). Gauge length set for testing was 1 inch and

crosshead speed was 18 mm min^{-1}. Denier of fibers was used to describe the fineness of keratin fibers. For each test, at least 20 specimens were used.

Qualitative measurement of disulfide bonds in keratin using Raman Spectroscopy

Feathers and keratin fibers were characterized on a Raman spectrometer (The DXR Raman microscope, Thermo, USA). The laser wavelength was set at 532 nm with a power of 10 mW. The exposure time for sample collection was 15 seconds with 15 cycles of exposures per sample. To compare the disulfide bonds in keratin, the ratio of peak areas around 500 cm^{-1} (S-S) and 1450 cm^{-1} (C-H) was used.

Quantification of cystine in fibers

Fibers collected from each step of the continuous spinning line were washed in distilled water followed by freeze-drying. The cystine content in fibers was determined based on the method developed by Campanella et al [35]. In detail, dried fibers were hydrolyzed using 6N HCl under 110 ^{o}C for 24 h to obtain amino acids. Phenylisothiocyanate was used for pre-column quantitative derivatization of amino acids by a HPLC, UltiMate 3000 series, USA equipped with a C8 column (Acclaim 120, 120 Å, 4.6 × 250 mm, 5 μm) and UV detector with wavelength set at 254 nm. The flow rate was 1 ml min^{-1} and a ternary gradient was employed using 0.7 M sodium acetate with pH 6.4 (phase A), water (phase B) and acetonitrile/water with a volume ratio of 8:2 (phase C). Gradient elution was used. Portion of phase A gradually decreased from 20% to 10%, phase B decreased from 75% to 10% while phase C increased from 5% to 80%. Total retention time was 30 min with an additional 10 min for column re-equilibration.

Determination of sulfur content

Sulfur content by Inductively Coupled Plasma Spectrometry (Agilent 7500 cx, Santa Clara, CA, USA) was determined. Around 50 milligrams of each sample were added in separate tubes before added 5X volume of nitric acid for sample digesting overnight at 70 ^{o}C. Finally, the samples were diluted 20 folds before injected into the autosampler.

Analysis of secondary structures

X-ray diffraction and solid ^{13}C NMR studies were carried out on for secondary structure analysis of feathers and keratin fibers. For X-ray diffraction was obtained using a Rigaku D/Max-B X-ray diffractometer with Bragg–Brentano parafocusing geometry, diffracted beam monochromator, and conventional copper target X-ray tube set (λ = 1.54 Å) to 40 kV and 30 mA at 26 °C. Diffraction intensities were recorded with 2θ ranging from 3° to 40° at a scan speed of 0.05° per second. The degree of crystallinity was calculated using Jade 6.0 software (Materials Data Incorporated: Livermore, CA, USA) with Gaussian peak fittings. The ^{13}C solid-state NMR spectra were obtained using a triple-resonance (1H/13C/15N) magic angle spinning probe (3.2 mm) was equipped on the NMR spectrometer (Bruker, Avance 600, USA). Smoothing, noise reduction and deconvolution were conducted using methods of Savitzky-Golay, Gassian and Line Fitting, respectively. These methods were included in the software of MestReNova 12.0.

Statistical analysis

One-way analysis of variance using the Scheffe test with a confidence interval of 95% was used for all obtained data. The statistical analysis was conducted on SAS 9.4 software (Cary, North Carolina) and survey procedures of PROC GLIMMIX.

Results and discussion

Controlled cleavage of disulfide bonds in keratin

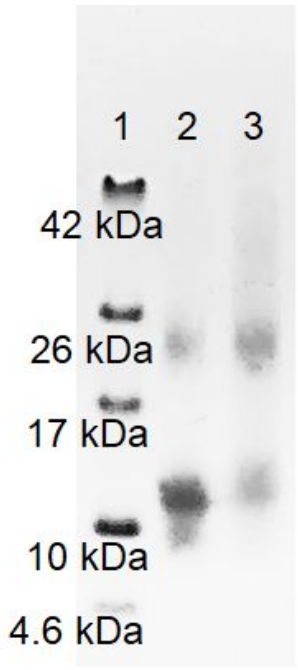

Figure 2 Reducing SDS-PAGE. Lane 1: standard protein markers; Lane 2: regenerated keratin; Lane 3: Chicken feathers

Figure 2 compares molecular weights of protein backbones between fibers and chicken feathers. The results show that damages to backbone of regenerated keratin were minimized. Compared to the chicken feather, contents of proteins with 21 kDa of regenerated keratin were slightly lower while contents of protein with molecular weight from 8 kDa and12 kDa were higher than those of chicken feathers. The results in Figure 2 also indicate that the regenerated keratin contained a high amount of γ-keratin, which has a molecular weight of 11 kDa [36] and contains high sulfur content. γ-keratin would facilitate formation of disulfide bonds in the process of fiber regeneration.

Table 1 Rheological properties of 18% keratin solution at 25 °C

Concentration of reducing agent (wt% based on keratin)	K value ($Pa•s^n$)	n value
0.5	18.90	0.97
1	14.23	0.97
2	4.19	0.91
3	1.50	0.95
4	1.31	0.96

K is the consistency coefficient, directly proportional to polymer viscosity. n is the flow behavior index. The smaller value of n indicates better molecular entanglement.

Table 1 shows the effect of different concentrations of reducing agents on the rheological properties of keratin spinning dope. The results show that cleavages of disulfide linkages directly affected the viscosity and entanglement of the keratin molecule in the solution. Specifically, as the concentration of the reducing agent increased, the viscosity of the solution gradually decreased, but the degree of molecular entanglement initially increased and then decreased. An increase in concentrations of reducing agent led to an increase in disulfide bonds cleaved. As a result, molecular weight of keratin gradually decreased, so did the viscosity. When the amount of the reducing agent increased from 0.5% to 2%, most ordered structures became uncoiled, leading to better solubility of keratin molecules. Therefore, the entanglement of molecules increased. When the concentration of the reducing agent continued to increase, the molecular weight was further lowered while the solubility of keratin remained unchanged. As a result, degrees of molecular entanglement decreased.

In order to ensure better spinnability of keratin fibers on a continuous spinning line, the disulfide bonds in keratin need to be partially retained because of the following three benefits. 1) Ensuring that the protein still had good solubility 2) Ensuring that the protein molecules were in highest entanglement 3) keeping the molecular weight of the protein high enough to allow the spinning dope to be solidified rapidly in the coagulation bath. Therefore, 2% reducing agent was selected to partially cleave disulfide linkages in the spinning dope.

Controlled assembly of disulfide bonds during the keratin fiber spinning

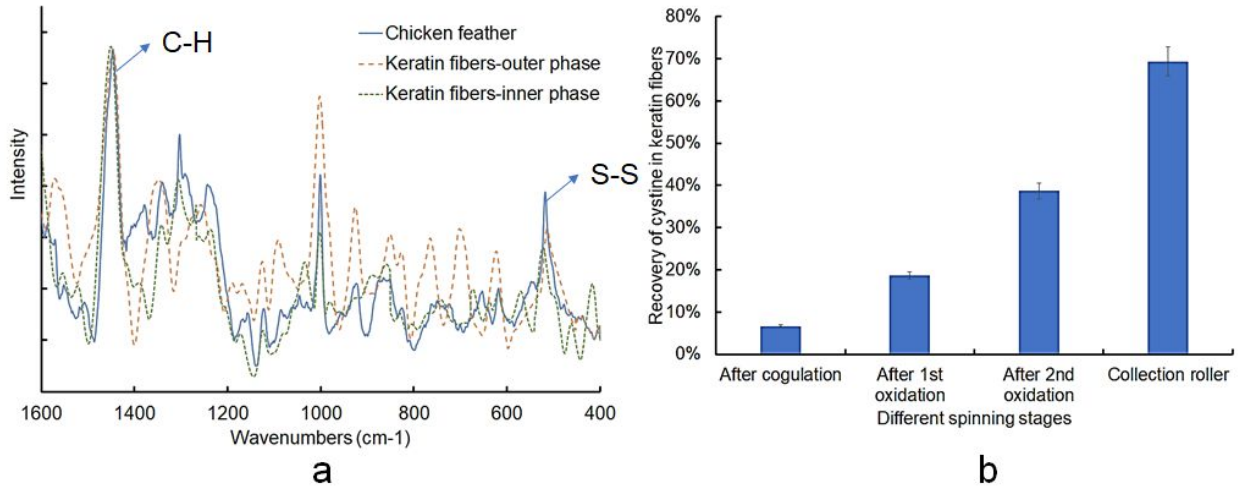

Figure 3 a) Comparison of disulfide bonds in keratin between chicken feathers and spun keratin fibers using Raman spectra. b) Recovery of disulfide bonds in keratin fibers measure by HPLC at different oxidation stages via controlled disulfide bond assembly.

Figure 3 shows the efficient recovery of disulfide bonds in keratin fibers via controlled disulfide bond assembly on a continuous spinning line and resultant spinnability of keratin fibers. The results show that the rapid establishment of disulfide crosslinkages in continuous spinning is an important factor ensuring the good spinnability of keratin fiber. Figure 3a qualitatively compares disulfide bonds in keratin fibers and chicken feathers. Results show that high degree of disulfide

crosslinkages was recovered in keratin fibers. The peaks at about 500 and 1450 cm^{-1} were S–S bonds and C–H bonds, respectively. The Raman spectra were normalized according to the C–H band, whose peak area was relatively large and not affected by the chemical treatments. Compared to the outer phase of fibers, the disulfide linkages in the inner phase of fibers were 14% lower based on the peaks fitting. The reason is that concentration of oxidant in fibers' outer phase was higher than that in fibers' inner phase during the spinning process. High concentration of oxidant helped form high degrees of disulfide linkages. However, due to the fine diameter of fibers, the oxidant can easily penetrate inner phase of fibers. Therefore, the difference in disulfide bond content between outer and inner phases of fibers was small. Disulfide linkages were quantified using HPLC. Figure 3b shows that less than 10% of the crosslinkage bonds in fibers were recovered in the coagulation bath. After initial drawing and first oxidation, nearly 20% of the disulfide bonds in the fiber were recovered. As further oxidations accompanied by fiber drawings, recovery degrees of disulfide linkages further increased. When fibers reached the final collection roller on a spinning line, nearly 70% of the disulfide bonds was recovered, with a degree of crosslinkages of about 5%. The rapid and high recovery in degrees of disulfide linkages in the continuous spinning process ensured good fiber spinnability. Changes in sulfur content during the process were also quantified. The sulfur contents in raw chicken feather, keratin extracts and spun fibers were 625, 943 and 522 μmmol L^{-1}. The increase in sulfur content in keratin extracts resulted from the addition of sulfur-containing reducing agents during the extraction. Some reducing agents were bonded to keratin after the formation of disulfide bonds with thiol groups on keratin. Possible reasons for the decrease in sulfur content in keratin fibers include beta elimination and lanthionine formation[23, 37] In spun fibers, sulfur content from cystine was 438 μmmol L^{-1} while sulfur content from cysteine was 89 μmmol L^{-1}. The rest 25

μmmol L^{-1} sulfur in spun fibers might be from lanthionine and disulfide bonds between cysteine and mercaptoethanol. The results indicate that more cystine could be formed with additional drawing and oxidation steps.

The spinnability of the fibers was substantially higher via fine control of disulfide bond assembly than that via random and simple control of disulfide bond assembly. Via controlled disulfide bond assembly, the final collection speed of the fiber reached 15 m min^{-1}, 160% of spinning using single-step oxidation in solution, 300% of spinning only with the air oxidation.

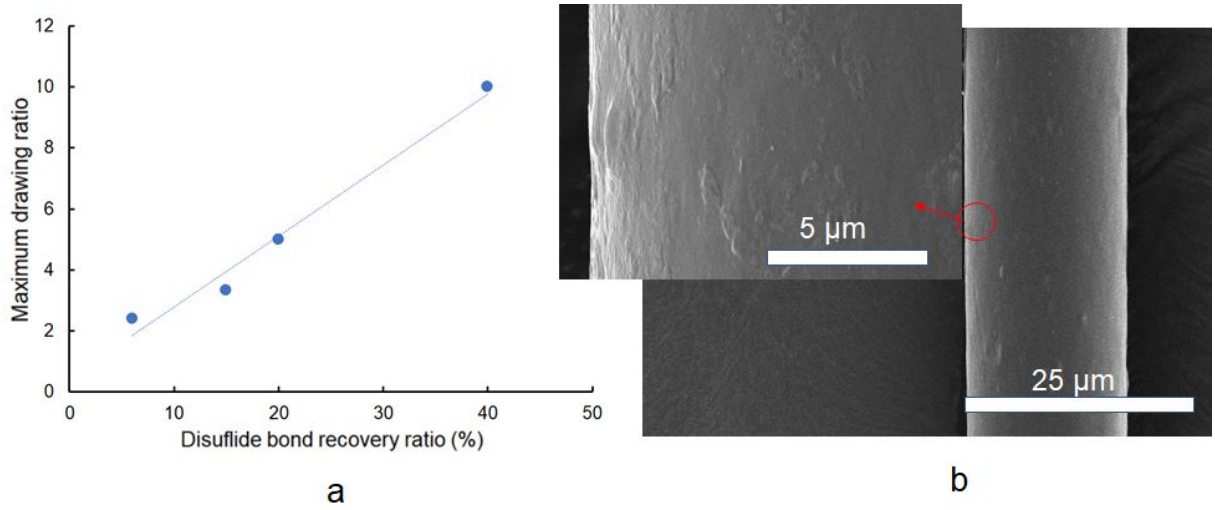

Figure 4 a) Relationship between recovery ratio of disulfide bonds in fibers and highest drawing ratio. b) Morphologies in SEM of spun keratin fiber from highest drawing ratio.

Figure 4a demonstrates a linear relationship between degree of crosslinkages in keratin fibers and maximum drawing ratios. Here, Maximum drawing ratio = 0.2* Disulfide bond recovery ratio + 0.5 with R^2 0.98. This result implies that recovery of disulfide linkages was the key to high drawing ratios of fibers. A high drawing ratio was a prerequisite for producing high-quality fibers. As shown in Figure 4a, when degrees of the disulfide bond recovery were less than 10%, the drawing ratio of the fiber was only 2 times. As recovery degree of disulfide bonds increased,

the maximum drawing ratio of the fiber increased to 10 times. The increase in draw ratio substantially reduced diameters of spun fibers. As shown in Figure 4b, fibers after 10 times of drawing had a diameter of around 15 μm, which is lower than most natural wool fibers (30 μm) [38] and slightly larger than silk fibers (10 μm) [39]. A magnified SEM image shows that the fiber surface was smooth. Fine fibers ensure a good hand, breathability, and dyeability. The results further indicate that continuous production of quality keratin fibers was heavily dependent on the rapid formation of crosslinkages via controlled disulfide bond assembly. Without controlled disulfide bond assembly, the recovery degree of the disulfide bond was not more than 20%, resulting in limited fiber draw ratios and subsequently poor fiber properties.

Figure S3 describes how high degrees of ordered protein structures were formed in keratin fibers via controlled disulfide bond cleavages and assembly under external stretch force. The distance between protein backbones in newly solidified fiber can be reduced to some extent because of the existence of limited disulfide linkages inside. The reduced distance between protein backbones facilitated the formation of intermolecular disulfide linkages during the first oxidation process. Then the newly formed crosslinkages helped to improve the fiber stretchability and drawing ratios. High drawing ratios contributed to the linearity of polymer chains in keratin fibers and thus decreased in distances between protein backbones. In turn, formation of intermolecular disulfide bonds was further facilitated. Via the controlled cleavage and assembly of disulfide bonds, intermolecular disulfide crosslinkages gradually increased and secondary structures were gradually recovered in keratin fibers. At collection step, last step of continuous line, fibers were once again oxidized to immobilize ordered structures of keratin.

Recovered secondary structure in keratin fibers

Table 2 Comparison of secondary structures between chicken feather and keratin fibers

Materials	Degree of crystallinity		
	Total crystallinity	Portion of α-helix	Portion of β-sheet
Chicken feathers	31%	11%	20%
Keratin fibers	24%	5%	19%

The data obtained from XRD and ^{13}C solid NMR. These spectra are shown in Figure S1. Raw NMR spectra are shown in Figure S2. Calculation of crystallinity was described in ESI.

Table 2 compares the secondary structure of keratin fibers with chicken feathers. The results showed that recovery of beta-sheet secondary structure and total crystallinity of keratin fibers were 95% and 80%, respectively. The high crystallinity in keratin fiber was due to the high degree of ordered structures resulting from controlled disulfide bonds cleavages and assembly. The reason for the high degree of beta-sheet recovery is as below. Controlled disulfide assembly contributed to the high stretchability of fibers and an increase in the fiber drawing ratios. Linear protein chains formed by high degrees of stretchability led to the formation of beta-sheet structures. The degree of crystallinity in keratin fiber was lower than that of the original chicken feathers mainly because the disulfide bond in the chicken feathers could not be completely recovered, and the ordered structures in keratin fibers were less than those in chicken feathers. In addition, slight damages on keratin backbone also contributed to the lower degree of crystallinity in keratin fibers.

Continuous spinnability from controlled disulfide cleavages and assembly

Supporting video demonstrates a bundle of keratin fibers was continuously produced via the controlled cleavage and assembly of disulfide bonds. The video demonstrated that multiple fibers

were extruded from the spinneret, passed through the coagulation bath, before reaching the final winding roller after 10 times of drawing ratio. Continuous fiber production with a good spinnability was also demonstrated.

Quality of keratin fibers

Table 3 Mechanical properties of keratin fibers compared to other common fibers.

Fiber source	Dry state			Wet state		
	Strength (Mpa)	Strain	Toughness (J cm^{-3})	Strength (Mpa)	Strain	Toughness (J cm^{-3})
Feather barbs[40]	161±27.5	9.7±3.3%	21±2	127±24.5	18±3%	31.5±3
Keratin fibers	**138±30.5**	**11±2.8%**	**18.5±2**	**81±23**	**25±3%**	**28.7±4**
Wool[41]	173±23	36±5%	32±5	140±22	46±5%	36±4
Cotton[12]	420±46	6.2±1.5%	10.5±5	472±34	9±1%	24.6±6
Line[12]	700±45	3.1±0.4%	5±1	800±40	5±1%	7±1
Viscose[12]	276±20	21±5.2%	24±6	120±20	25±4%	21.1±4.3

Our work is shown in **bold** font.

Table 3 shows the mechanical properties of the fibers with restored secondary protein structures and compares properties of keratin fibers with other common fibers. The results show that keratin fibers recovered 86% of stress properties at dry state, 64% of wet stress, 89% of dry toughness and 91.55% of wet toughness of original chicken feathers. Typical stress-strain curves for keratin fibers and feathers are included in Figure S4. The stress and strain for keratin fibers

were lower and higher than feathers, respectively. Lower degrees of crystallinity and disulfide crosslinkages resulted in the lower stress of keratin fibers. As a result, stress at *oa* stage in keratin fibers was lower than the stress of feathers. Also, due to the low degrees of crystallinity, crosslinkages, and molecular linearity, molecular chains were flexible in keratin fibers. In addition, substantial disulfide bonds were recovered in keratin fibers, increasing the length of molecular chains. Because of flexible but long molecular chains, relative slippage between molecular chains could be facilitated. As a result, a stage (*ab*) which played the major role in fibers' flexibility appeared in the curve of keratin fibers. Keratin fibers had merits among other commonly used fibers. For example, keratin strain and toughness were substantially higher than cotton and linen. The toughness was close to viscose fibers. The above results show that keratin fibers with restoration of secondary structures from continuous production meet the requirements for practical uses.

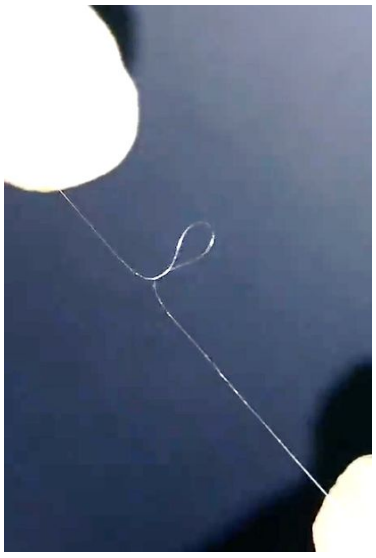

Figure 5 Keratin filament endured a high degree of twisting.

Figure 5 shows that keratin fibers can endure a high degree of twisting. Supporting videos further demonstrate the high ductility of keratin fiber. The fiber ductility was high because of the high

toughness of the fiber, stemming from substantial restoration of the secondary protein structures via controlled disulfide bond cleavage and assembly in the continuous spinning process.

Table 4. Comparison of properties of regenerated keratin fibers developed from various approaches.

Approach to regeneration	Properties recovery	Continuous production on pilot scale	Reference
Controlled disulfide cleavage and assembly	**86% of tenacity 113% of strain**	**Yes**	**This work**
Control of disulfide cleavages	48% of tenacity 41% of strain	No	[27]
Applied glycerol as plasticizer	4% of tenacity 280% of strain	No	[42]
Blend poly(ethylene oxide) (containing 10% keratin)	3% of tenacity 1100% of strain	No	[43]

Property recovery based on the original keratin materials, such as feathers and wool.

Table 4 compares the properties of keratin fibers from various regeneration approaches. All keratin fibers except this work were regenerated on a lab-scale. Results show that due to the low recovery of secondary structures, tenacity recovery was low, with the highest still less than 50%. With poor recovery of secondary structure, the breaking strain of regenerated fibers was even poor. To increase the breaking strain, incorporation of plasticizer or other polymers into keratin was developed. As a result, the breaking strain increases at the cost of sacrifice of fiber tenacity.

For example, after incorporation of glycerol, the tenacity of regenerated keratin fibers was only 4% of raw fibers.

Cost-effective production with limited environmental impact

Keratin content in continuous spun fibers was higher than 98%, indicating the full degradability of fibers. In order to estimate market potential of the regenerated keratin fibers, the material consumption and costs in our method are assessed, as shown in Table S2. Total material costs to produce 1 kg of keratin fibers was about $0.83. Compared to the bulk price (metric ton scale) of wool at about $7-30 kg^{-1} and silk at about $45-80 kg^{-1}, keratin fibers from chicken feathers had their cost at least 91% lower than sale prices. Considering other costs in large-scale production, the final price of keratin fibers from chicken feathers would be competitive. If keratin fibers from poultry feathers are sold at about $4 kg^{-1}, which is close to some natural cellulose fibers like linen, a ton of poultry feathers would produce fibers worth at least $3,000. If 5 million tons of poultry feathers worldwide could be fully exploited, the market value of regenerated keratin fibers would exceed $10 billion.

Current spinning technology still needs improvement for the green process. For example, HCl and NaOH could be neutralized before discharge. However, salts after neutralization still need to be addressed. Though some studies show that SDS is considered biodegradable[44], toxicity to aquatic organisms brought by SDS is still a concern especially given that a high amount of SDS was used in this work. In the future, we need to keep exploring nontoxic, sustainable and degradable alternatives to replace current additives. Some other technologies must be applied for full reuse of coagulation bath. Though there was no significant difference in properties of spun fibers after reusing coagulation bath by adjusting pHs on a pilot scale, constant accumulation of residuals from spinning dopes such as SDS would finally affect the fibers' spinnability and

property. Membrane technology is one of green and sustainable processes suitable for continuous production for the removal of impurities and reuse of baths [45]. After achieving complete reuse of baths, chemicals, additives, the spinning technology can realize minimal discharges and environmental impact.

Conclusion

Regenerated quality keratin fibers have been successfully continuously produced on a pilot scale. Via controlled cleavage and assembly of disulfide crosslinkages in keratin on the continuous production line, total crystallinity, beta-sheet crystallinity and disulfide crosslinkages in keratin fibers were recovered 78%, 95% and 71%, respectively, compared to chicken feathers. Because of the efficient secondary structure recovery, keratin was continuously spun into fine fibers with a diameter of 15 μm and 86%, 64%, 89% and 91% recoveries in dry tenacity, wet tenacity, dry toughness and wet toughness, respectively. Though chemicals selected in this work were based on safety, non-toxicity and degradability, we still need to explore greener and safer and more biodegradable chemicals and additives towards a complete green spinning process. For instance, alternative options must be explored to replace the use of current acid, alkali and additives such as SDS. The processing temperature could be further lowered to conserve energy.

Acknowledgment

The research has been supported by the Nebraska Environmental Trust (NET Grant 18-116), the United States Department of Agriculture National Institute of Food and Agriculture (award number 2019-67021-29940) and the Agricultural Research Division at the University of Nebraska-Lincoln. The research was performed in part in the Nebraska Nanoscale Facility: National Nanotechnology Coordinated Infrastructure and the Nebraska Center for Materials and

Nanoscience, which are supported by the National Science Foundation under Award ECCS: 1542182, and the Nebraska Research Initiative. Bingnan is grateful to the John and Louise Skala Fellowship and AATCC Students Grant for their financial support. Faqrul is grateful to Dr. Joan Laughlin Fellowship. Special thanks to Angel Torres and Jehad Abourahma in Dr. Alexander Sinitskii's group for their assistance in Raman Spectroscopy.

Conflicts of interest

There are no conflicts to declare.

Reference

1. Y. Zhang, N. Du, Y. Chen, Y. Lin, J. Jiang, Y. He, Y. Lei and D. Yang, *Nanoscale*, 2018, **10**, 5626-5633.
2. A. G. Nandgaonkar, Q. Wang, K. Fu, W. E. Krause, Q. Wei, R. Gorga and L. A. Lucia, *Green Chemistry*, 2014, **16**, 3195-3201.
3. Y. Li, H. Liu, J. Song, O. J. Rojas and J. P. Hinestroza, *ACS applied materials & interfaces*, 2011, **3**, 2349-2357.
4. B. Mu, H. Xu, W. Li and Y. Yang, *Bioresource technology*, 2019, **273**, 305-312.
5. J. K. Pandey, S. Ahn, C. S. Lee, A. K. Mohanty and M. Misra, *Macromolecular Materials and Engineering*, 2010, **295**, 975-989.
6. B. Mu, H. Xu and Y. Yang, *Bioresource Technology*, 2015, **196**, 332-338.
7. H. A. Le Phuong, N. A. Izzati Ayob, C. F. Blanford, N. F. Mohammad Rawi and G. Szekely, *ACS Sustainable Chemistry & Engineering*, 2019, **7**, 11885-11893.
8. N. A. Nguyen, K. Kim, C. C. Bowland, J. K. Keum, L. T. Kearney, N. André, N. Labbé and A. K. Naskar, *Green Chemistry*, 2019, **21**, 4354-4367.
9. Y. Ma, B. Zeng, X. Wang and N. Byrne, *ACS Sustainable Chemistry & Engineering*, 2019, **7**, 11937-11943.
10. Z. Yang, A. Kumar, A. W. Apblett and A. M. Moneeb, *Green Chemistry*, 2017, **19**, 757-768.
11. Industrievereinigung-Chemiefaser, Worldwide production volume of chemical and textile fibers from 1975 to 2016 (in 1,000 metric tons), https://www-statista-com.libproxy.unl.edu/statistics/263154/worldwide-production-volume-of-textile-fibers-since-1975/ (accessed 7/7, 2018).
12. N. Reddy and Y. Yang, *Green Chemistry*, 2005, **7**, 190-195.
13. G. Gao, M. A. Karaaslan, J. F. Kadla and F. Ko, *Green Chemistry*, 2014, **16**, 3890-3898.
14. B. Mu, H. Xu, W. Li, L. Xu and Y. Yang, *Food Hydrocolloids*, 2019, **90**, 443-451.
15. B. Mu, W. Li, H. Xu, L. Xu and Y. Yang, *Journal of Materials Chemistry A*, 2018, **6**, 10320-10330.
16. F. Allievi, M. Vinnari and J. Luukkanen, *Journal of Cleaner Production*, 2015, **92**, 142-151.
17. L. Gao, H. Hu, X. Sui, C. Chen and Q. Chen, *Environmental science & technology*, 2014, **48**, 6500-6507.
18. N. Reddy, L. Chen, Y. Zhang and Y. Yang, *Journal of Cleaner Production*, 2014, **65**, 561-567.

19. A. J. Poole, J. S. Church and M. G. Huson, *Biomacromolecules*, 2008, **10**, 1-8.
20. K. M. ARAI, R. TAKAHASHI, Y. YOKOTE and K. AKAHANE, *European journal of biochemistry*, 1983, **132**, 501-507.
21. C. Tonin, A. Aluigi, C. Vineis, A. Varesano, A. Montarsolo and F. Ferrero, *Journal of thermal analysis and calorimetry*, 2007, **89**, 601-608.
22. K. Ziegler, *Journal of Biological Chemistry*, 1964, **239**, PC2713-PC2714.
23. W. Crewther, L. Dowling, A. Inglis and J. Maclaren, *Textile research journal*, 1967, **37**, 736-745.
24. N. Singh and K. Prasad, *Green Chemistry*, 2019, **21**, 3328-3333.
25. S. Zheng, Y. Nie, S. Zhang, X. Zhang and L. Wang, *ACS Sustainable Chemistry & Engineering*, 2015, **3**, 2925-2932.
26. K. Kammiovirta, A.-S. Jääskeläinen, L. Kuutti, U. Holopainen-Mantila, A. Paananen, A. Suurnäkki and H. Orelma, *RSC Advances*, 2016, **6**, 88797-88806.
27. H. Xu and Y. Yang, *ACS Sustainable Chemistry & Engineering*, 2014, **2**, 1404-1410.
28. R. Wormell and F. Happey, *Nature*, 1949, **163**, 18.
29. J. G. Rouse and M. E. Van Dyke, *Materials*, 2010, **3**, 999-1014.
30. Y. Li, X. Zhi, J. Lin, X. You and J. Yuan, *Materials Science and Engineering: C*, 2017, **73**, 189-197.
31. N. V. Patil and A. N. Netravali, *ACS Omega*, 2019, **4**, 5392-5401.
32. J. Li, Y. Li, L. Li, A. F. Mak, F. Ko and L. Qin, *Polymer Degradation and Stability*, 2009, **94**, 1800-1807.
33. O. Thomas and G. White, *Biotechnology and applied biochemistry*, 1989, **11**, 318-327.
34. X. Mi, H. Xu and Y. Yang, *Colloids and Surfaces B: Biointerfaces*, 2019, **177**, 33-40.
35. L. Campanella, G. Crescentini and P. Avino, *Journal of Chromatography A*, 1999, **833**, 137-145.
36. T. Posati, D. Giuri, M. Nocchetti, A. Sagnella, M. Gariboldi, C. Ferroni, G. Sotgiu, G. Varchi, R. Zamboni and A. Aluigi, *European Polymer Journal*, 2018, **105**, 177-185.
37. S. Blackburn and G. Lee, *Biochimica et biophysica acta*, 1956, **19**, 505-512.
38. N. Reddy and Y. Yang, *Innovative bio bers from renewable resources*, Springer, 2015.
39. K. M. Babu, in *Silk (Second Edition)*, ed. K. M. Babu, Woodhead Publishing, 2019, DOI: https://doi.org/10.1016/B978-0-08-102540-6.00003-6, pp. 51-75.
40. N. Reddy and Y. Yang, *Journal of Polymers and the Environment*, 2007, **15**, 81-87.
41. N. Reddy and Y. Yang, *Innovative biofibers from renewable resources*, Springer, Berlin, Heidelberg, 2015.
42. B. Ma, X. Qiao, X. Hou and Y. Yang, *International journal of biological macromolecules*, 2016, **89**, 614-621.
43. A. Aluigi, C. Vineis, A. Varesano, G. Mazzuchetti, F. Ferrero and C. Tonin, *European Polymer Journal*, 2008, **44**, 2465-2475.
44. C. A. Bondi, J. L. Marks, L. B. Wroblewski, H. S. Raatikainen, S. R. Lenox and K. E. Gebhardt, *Environmental health insights*, 2015, **9**, EHI. S31765.
45. M. Razali, J. F. Kim, M. Attfield, P. M. Budd, E. Drioli, Y. M. Lee and G. Szekely, *Green Chemistry*, 2015, **17**, 5196-5205.